Cation Distribution in a Series of Mixed Ferrites $Mg_xMn_{1.1-x}Sn_{0.1}Fe_{1.8}O_4$ by Means of Powder X-Ray Diffraction and ^{57}Fe, ^{119}Sn Mössbauer Spectroscopy

Koji YAMADA,* Hiroyuki OHSHITA, Shinya FUNABIKI,
Hiroshi SAKAI, and Sumio ICHIBA
Department of Chemistry, Faculty of Science, Hiroshima University,
Higashisenda-machi, Naka-ku, Hiroshima 730
(Received May 28, 1990)

The cation distribution in a series of $Mg_xMn_{1.1-x}Sn_{0.1}Fe_{1.8}O_4$ spinel ferrites has been studied by means of X-ray powder diffraction and ^{57}Fe, ^{119}Sn Mössbauer spectroscopy. All of these ferrites showed broad ^{119}Sn Mössbauer spectra due to the hyperfine magnetic field from the ferrimagnetically ordered cations at the A and B sites. With increasing x the distribution of the hyperfine field at the Sn atom became broader and the hyperfine field decreased abruptly above x=0.825. This observation indicates that diamagnetic Mg^{2+} ions are excluded from the A site below x=0.55, but occupy the A site as well as the B site only above x=0.825. This result is consistent with the Rietveld analyses of the X-ray powder diffraction data. The ^{119}Sn Mössbauer spectroscopy is shown to be a useful technique for studying the cation distribution of ternary spinels in which the site preference of cations can not be empirically predicted.

Magnesium-manganese mixed ferrites, $Mg_xMn_{1-x}Fe_2O_4$ (X=0 to 1), have been widely used for many technological applications owing to their electric, magnetic, and catalytic properties. These properties are, however, to a large extent determined by the cation distribution in the ferrite lattice. These ferrites have spinel structures generally represented by the chemical formula MM'_2O_4, where M and M′ are divalent and trivalent cations. The structure consists of a face-centered cubic close-packed array of oxide anions with M and M′ ions occupying one eighth of the tetrahedral (A site) and one half of the octahedral interstices (B site). There are two extreme cation distributions, i.e. normal and inverse spinels which are traditionally represented as $(M)[M']_2O_4$ and $(M')[MM']O_4$, respectively. The cation distributions in binary ferrites have been extensively studied and have been found to be affected by several factors such as the Madelung energy and the crystal field stabilization energy. In a binary ferrite, $(M_xFe_{1-x})[M_{1-x}Fe_{1+x}]O_4$, the cation distribution is derived from the minimum of the Gibbs free energy and is expressed as follows:[1-6]

$$x(1+x)/(1-x)^2 = \exp(-\Delta H/RT),$$

where ΔH is the enthalpy difference between normal (x=1) and inverse (x=0) spinel ferrites.

For ternary spinels, however, the cation distribution is a complicated problem. For example, the Mg^{2+} ion distribution in ternary spinels can not be simply predicted only from the above factors. H. V. Kiran et al.[7] suggested that the Mg^{2+} ion distribution over the A and B sites in a binary spinel was modified by the addition of the third cations because of the large diffusibility of the Mg^{2+} ion. The cation distributions in the $MgFe_2O_4$ and $MnFe_2O_4$ ferrites, quenched from sintering temperatures, have been reported as $(Mg_{0.25}Fe_{0.75})[Mg_{0.75}Fe_{1.25}]O_4$ and $(Mn_{0.8}Fe_{0.2})[Mn_{0.2}Fe_{1.8}]O_4$, respectively.[8-10]

In this study we investigated the cation distribution of the solid solutions, $Mg_xMn_{1.1-x}Sn_{0.1}Fe_{1.8}O_4$, by means of the Rietveld analysis of the powder X-ray data and discuss how the hyperfine fields of the Sn and Fe atoms are influenced by the cation distribution. ^{119}Sn Mössbauer spectroscopy is particularly useful for studying the cation distribution if a diamagnetic Sn^{4+} ion is introduced in the ferrite lattice. This is due to the fact that the diamagnetic ion is subjected only to the supertransferred or transferred hyperfine magnetic fields which reflect the number and kind of cations in the nearest neighbors.[11-13]

Experimental

A series of ferrites, $Mg_xMn_{1.1-x}Sn_{0.1}Fe_{1.8}O_4$ (X=0 to 1.1 in a step of 0.275), was prepared in their polycrystalline forms by a double-sintering process in air at 1000 and 1380 °C for 10—20 h using stoichiometric amounts of oxides. Each sample was rapidly quenched in water from the sintering temperature. In order to introduce aliovalent Sn^{4+} as a Mössbauer probe into the ferrite lattice, the electric charge was compensated as $2\,Fe^{3+}=Sn^{4+}+Mn^{2+}$ (or Mg^{2+}). Powder X-ray diffraction was observed with a Rigaku diffractometer (Rad-B system) in the range $10°<2\theta<90°$ at a sampling step of 0.01° using Ni-filtered Cu $K\alpha$ radiation. Each specimen was confirmed as being a single-phase spinel. The structural parameters of the cubic spinel, such as the lattice constant, oxygen u parameter, and occupation factor of the Mg^{2+} ion on the A and B sites were deduced by means of the Rietveld method using a Fortran program developed by Izumi.[14,15] The ^{57}Fe and ^{119}Sn Mössbauer spectra were measured using a constant-acceleration type spectrometer. The gamma-ray sources of ^{57}Co in a Rh matrix and ^{119m}Sn in $CaSnO_3$ were used at room temperature. The velocity scales for the spectrometers were calibrated with α-Fe for ^{57}Fe and $BaSnO_3$ and β-Sn for ^{119}Sn. The ^{57}Fe Mössbauer spectra were analyzed with Lorentzian curves by a least-squares method. The distribution of the hyperfine magnetic field at the Sn sites

was obtained from the ^{119}Sn Mössbauer spectrum by means of the Hesse and Rubartsch method.[16]

Results and Discussion

Rietveld Analysis of the Powder X-Ray Diffraction Data. The cubic lattice constants, which were refined by a Rietveld analysis mentioned below, are plotted in Fig. 1(A) against x for a series of ferrites. The lattice constants of these ferrites, in which 10 atomic % of iron atoms are substituted for tin atoms, increase by about 0.4% compared to that of pure Mn- or Mg- ferrite. This fact suggests an incorporation of tin atoms into the ferrite lattice. Though the lattice constant decreased with increasing x according to Vegard's law, only a slight change of the slope was detected between x=0.55 and 0.825. This slight change was probably due to a drastic change in the Mg^{2+} ion distribution (described latter).

In order to discuss the cation distribution quantitatively in terms of an X-ray technique, a full-profile refinement method of the diffraction pattern (Rietveld analysis) is very suitable. Although it was impossible regarding this Mg–Mn ferrite to distinguish Mn^{2+} from isoelectronic Fe^{3+} by an X-ray technique, the site occupancy of the Mg^{2+} ion could be successfully determined. In these refinements tin atoms were assumed to occupy the B site substitutionally according to previous study on Mg ferrite.[17] A cubic spinel with the formula MM'_2O_4 has a space group O_h^7 (*Fd3m*, No. 227); M and M′ occupy fixed 8(a) and 16(d) positions (Wykoff notation), respectively. Then, the structural parameters which should be determined are the lattice constant, the oxygen u parameter (32(e): (u,u,u)), the thermal parameters, and the cation distribution on the A and B sites. In order to determine the site occupancy of Mg^{2+}, a minimum point of the R_F values was searched as a function of the mole fraction of Mg^{2+} (y) on the A site following a precise determination of the base-line function and the line-shape profile function. Figure 2 shows the final result of a Rietveld analysis for x=0.825; Figure 3 shows a plot of the R_F values against y for each ferrite. The final structural parameters for a series of ferrites are listed in Table 1, where the same overall isotropic thermal parameters were assumed for all of these ferrites since, in some cases, they could not be refined independently. As is apparent from this Table, the

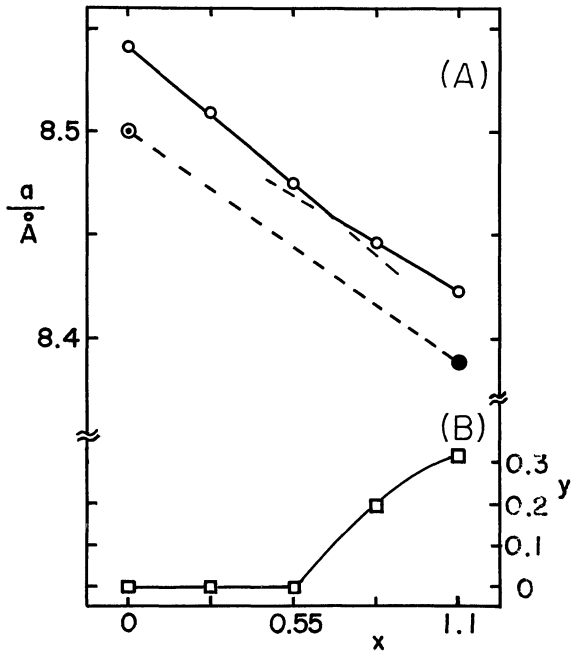

Fig. 1. (A) Cubic lattice constants (a) versus x for a series of $Mg_xMn_{1-x}Sn_{0.1}Fe_{1.8}O_4$ and (B) occupation factor (y) of Mg^{2+} ion on the A site versus x. ●: $MgFe_2O_4$, ⊙: $MnFe_2O_4$, cited from ASTM cards (36-398, 10-319).

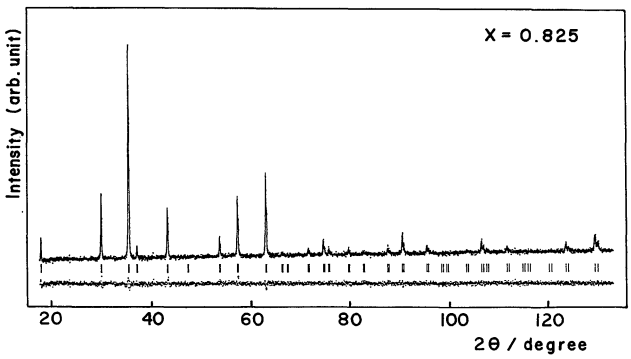

Fig. 2. Rietveld analysis for $Mg_{0.825}Mn_{0.275}Fe_{1.8}Sn_{0.1}O_4$. The solid line is the best-fit profile and the points are raw data. The difference between them are shown at the bottom.

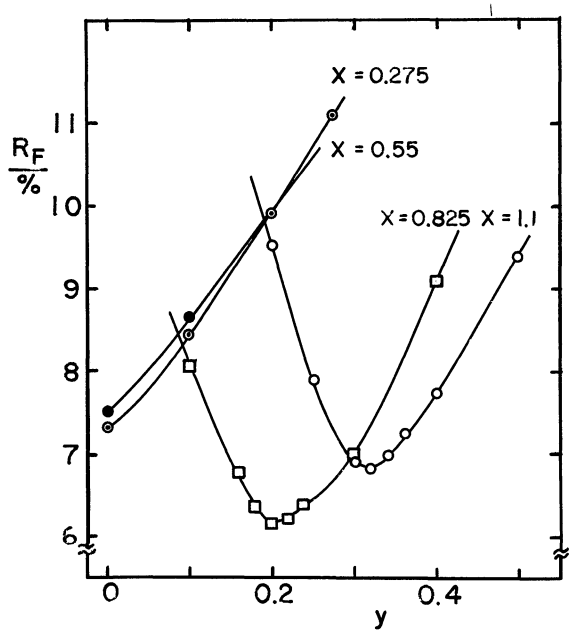

Fig. 3. Dependence of R_F values on the occupation factors (y) for a series of $Mg_xMn_{1-x}Sn_{0.1}Fe_{1.8}O_4$.

Mg^{2+} ions are perfectly excluded from the A sites for x=0, 0.275, and 0.55, whereas they occupy the A sites, as well as B, only for x=0.825 and 1.1, as is shown in Fig. 1(B). In the case of the x=1.1 sample parameter y is 0.32 and is considerable higher than the value reported previously.[9] The fraction of Mg^{2+} ions occupying the A sites, however, is 0.29 (Mg(A)/(Mg(A)+Mg(B))=0.32/1.1), which is slightly smaller than a prediction from the high-temperature limit (a random distribution: Mg(A)/(Mg(A)+Mg(B))=1/3. It is interesting to note that the abrupt change of the cation distribution clearly affects their lattice constants at this point (Fig. 1).

Table 1. Structural Parameters for a Series of $Mg_xMn_{1-x}Sn_{0.1}Fe_{1.8}O_4$[a,b]

x	R_F/%[c]	a/Å	u parameter	y[d]
0	6.2	8.542(1)	0.3842(5)	0
0.275	7.3	8.509(1)	0.3839(5)	0.00(2)
0.55	7.5	8.475(1)	0.3838(5)	0.00(2)
0.825	6.2	8.446(1)	0.3811(5)	0.20(2)
1.1	6.8	8.423(1)	0.3811(5)	0.32(2)

a) A site: 8(a) (0,0,0), B site: 16(d) (5/8,5/8,5/8) and Oxygen: 32(e) (u,u,u). b) Overall isotropic thermal parameters were assumed to be 0.5 Å^2. c) $R_F=\sum|I(o)^{1/2}-I(c)^{1/2}|/\sum I(o)^{1/2}$. d) y: Mole fraction of Mg^{2+} ion on the A site.

^{57}Fe Mössbauer Spectroscopy. Figure 4 shows the ^{57}Fe Mössbauer spectra for a series of $Mg_xMn_{1.1-x}Sn_{0.1}Fe_{1.8}O_4$ ferrites at room temperature. The spectra were analyzed with two sets of sextets corresponding to ^{57}Fe nuclei in the A and B sublattices, according to the assignments reported in previous papers.[8,9,18,19] In these calculations no quadrupole splitting and the same line-width parameters for the two sextets were assumed because of the strong overlapping of the A and B sites. The ^{57}Fe Mössbauer parameters obtained from the fitting are given in Table 2. The values of the isomer shift (IS) shows no composition dependence within the experimental errors and are characteristic of

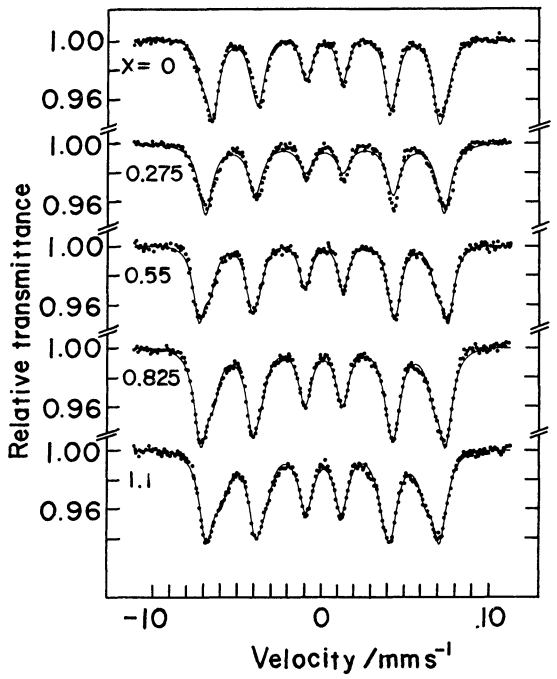

Fig. 4. ^{57}Fe Mössbauer spectra for a series of $Mg_xMn_{1.1-x}Sn_{0.1}Fe_{1.8}O_4$ at 298 K.

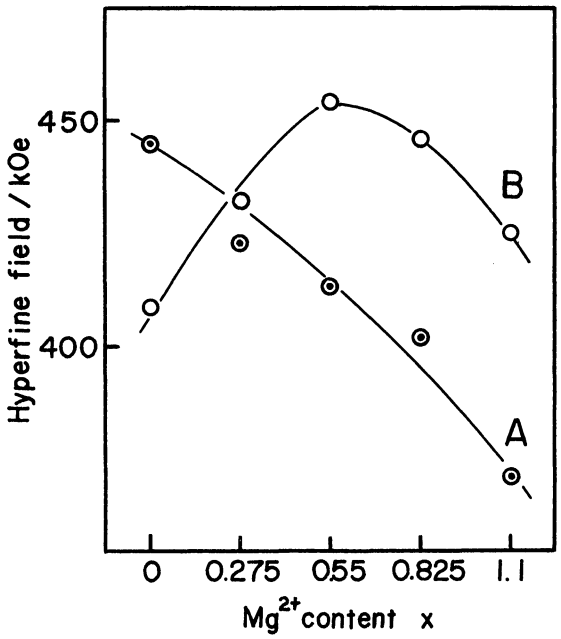

Fig. 5. ^{57}Fe Hyperfine fields at the A and B sites, H_{hf}(A) and H_{hf}(B), are plotted against x for a series of $Mg_xMn_{1-x}Sn_{0.1}Fe_{1.8}O_4$.

Table 2. ^{57}Fe Mössbauer Parameters for a Series of a $Mg_xMn_{1-x}Sn_{0.1}Fe_{1.8}O$ at 298 K[a,b]

x	H_{hf}(A), H_{hf}(B)	IS(A), IS(B)	Line width
	kOe	mm s^{-1}	mm s^{-1}
0	445(483), 410(430)	0.20, 0.26	0.83
0.275	423, 432	0.16, 0.23	1.00
0.55	413(441), 454(474)	0.22, 0.18	0.83
0.825	402, 446	0.20, 0.16	0.94
1.1	371(464), 425(496)	0.19, 0.15	1.03

a) Parameters in parentheses correspond to $Mg_xMn_{1-x}Fe_2O_4$ (x=0, 0.5, and 1) reported in Ref. 10, 19, and 18. b) Oe=1000/4π A m^{-1}.

high-spin Fe^{3+} ions. In the $Mn_{1.1}Fe_{1.8}Sn_{0.1}O_4$ ferrite, as is shown in Fig. 4, weak shoulders assigned to Fe^{3+} at A site have a larger hyperfine field than of the B site. In $Mg_{1.1}Fe_{1.8}Sn_{0.1}O_4$, however, these weak shoulders assigned to the A site appeared at the opposite side, suggesting a crossover of the hyperfine field with x. These observation are qualitatively consistent with previous data for $MnFe_2O_4$, $MgFe_2O_4$, and mixed ferrites,[8,9,18,19] except for a systematical decrease in the hyperfine field due to the high concentration of diamagnetic tin atoms. The hyperfine filed at the A and B sites are plotted against x in Fig. 5. The hyperfine field at the A site linearly decreases with increasing x, whereas that at B site indicates a maximum at x=0.55. This behavior of the B site is quite similar to that observed in the ^{119}Sn Mössbauer effect as will be stated below.

^{119}Sn Mössbauer Spectra for $Mg_xMn_{1.1-x}Sn_{0.1}Fe_{1.8}O_4$. The ^{119}Sn Mössbauer spectra for the $Mg_xMn_{1.1-x}Sn_{0.1}Fe_{1.8}O_4$ ferrites at 110 K are shown in Fig. 6 together with the distributions of the hyperfine field. Because of the ferrimagnetic property of these ferrites, two kinds of cations (Fe^{3+} and Mn^{2+}) are magnetically ordered in the spinel sublattices. These broad spectra are, therefore, attributable to the transferred hyperfine magnetic field from the cations at the A and B sites. The extremely broad distributions of $H_{hf}(Sn)$ are partly due to the high Sn^{4+} contents in these ferrites by considering the spectra of the ferrites containing less Sn^{4+} content.[12] The variation of the respective hyperfine field, which was determined to be a maximum of the single Gaussian curves estimated by a least-squares method, are plotted against x in Fig. 7. In the case of Mn-ferrite, the hyperfine field well agreed with the value reported by Lyubutin et al.[12] Regarding Mg-ferrite, however, $H_{hf}(Sn)$ estimated from Fig. 6(B) is about 20 kOe (1 Oe=1000/4 πA m^{-1}) and smaller than previous data ($H_{hf}(Sn)$=48±15 kOe).[20] This discrepancy is probably due to a difference in the cation distribution, since our sample was prepared by rapid cooling from high temperature, and also had a high Mg concentration (x=1.1).

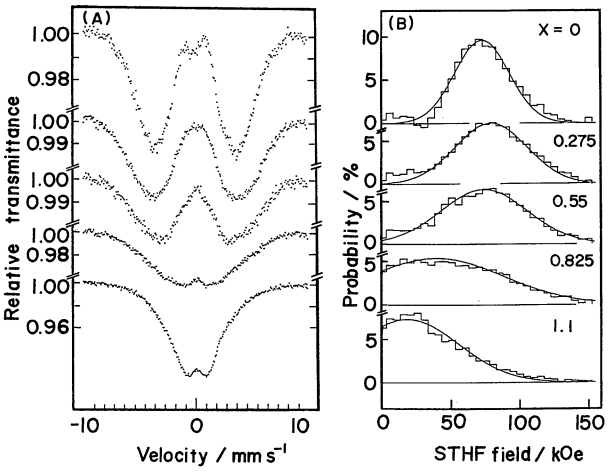

Fig. 6. ^{119}Sn Mössbauer spectra and the distributions of the transferred hyperfine magnetic field for a series of $Mg_xMn_{1-x}Sn_{0.1}Fe_{1.8}O_4$ at 110 K.

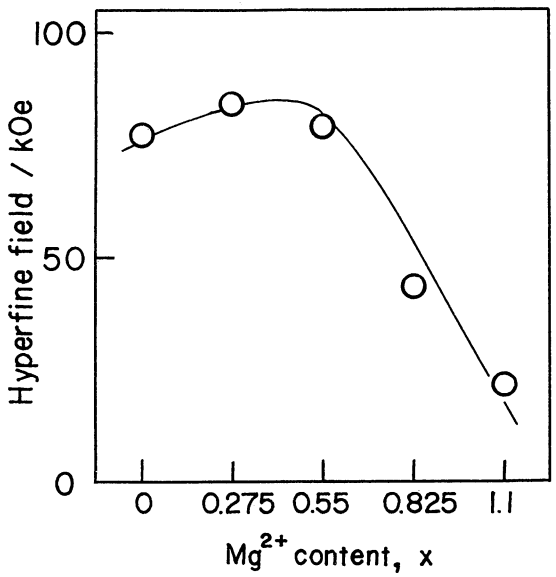

Fig. 7. Transferred hyperfine magnetic field at the ^{119}Sn nuclei, $H_{hf}(Sn)$, versus x for a series of $Mg_xMn_{1-x}Sn_{0.1}Fe_{1.8}O_4$.

Cation Distribution and $H_{hf}(Sn)$. The hyperfine magnetic field at the diamagnetic Sn atom, $H_{hf}(Sn)$, provides us with usuful chemical information since it is sensitive to the nearest neighbors at A and B sites. In the spinel ferrite $H_{hf}(Sn)$ is semiempirically expressed as two complementary mechanisms from the A and B sites,[12,21]

$$H_{hf}(Sn) = m H_A + n H_B, \quad (1)$$

where H_A and H_B are a supertransferred hyperfine (STHF) field through one A–O–B bond and a direct transferred field from one of the nearest magnetic ions in the B sites; m and n are the numbers of magnetic nearest neighbors. The most probable m and n can be deduced from the maximum probability given by the binomial law. For example, the probability of an Sn atom having m magnetic nearest neighbors at the A-site, $P(m)$, is expressed as

$$P(m) = {}_6C_m(1-y)^m y^{6-m}, \quad (2)$$

where y is the mole fraction of the diamagnetic Mg^{2+} on A site. Shigematsu et al applied these formula to isostructural Fe_3O_4 and γ-Fe_2O_3 and estimated the transferred field from the Fe^{3+} at the A and B sites to be −117 and 113 kOe/atom, respectively.[22] The supper-transferred hyperfine field from Mn^{2+}, on the other hand, was estimated to be about 60% of the corresponding Fe(A)–O–Sn(B).[13] It should be emphasized here

that in the spinel structure there are two times as many B sites as there are A sites. That is, the variation of the cation distribution affects more remarkably m than n. Using the cation distributions (Table 1) and Eq. 2, though the averaged values for m are estimated to be 6 between x=0 to 0.55, it decreased to 4.1 at x=1.1. This is consistent with the abrupt decrease of H_{hf}(Sn) above x=0.825.

References

1) A. Navrotsky and O. J. Kleppa, *J. Inorg. Nucl. Chem.*, **29**, 2701 (1967).
2) C. Glidewell, *Inorg. Chim. Acta.*, **19**, L45 (1976).
3) J. K. Burdett, G. D. Price, and S. L. Price, *J. Am. Chem. Soc.*, **104**, 92 (1982).
4) C. O. Arean and J. S. D. Vinuela, *J. Solid State Chem.*, **60**, 1 (1985).
5) A. N. Cormack, G. V. Lewis, S. C. Parker, and C. R. A. Catlow, *J. Phys. Chem. Solid.*, **49**, 53 (1988).
6) S. Kurpicka and P. Novak, "Ferromagnetic Materials," ed by E. P. Wohlfarth, North-Holland Publishing Company (1982), Vol. 3 p. 189.
7) H. V. Kiran, K. Seshan, and D. K. Chakrabarty, *J. Solid State Chem.*, **41**, 63 (1982).
8) G. A. Sawatzky, F. van der Woude, and A. H. Morrish, *Phys. Rev.*, **187**, 747 (1969).
9) J. H. Hastings and L. M. Corlies, *Phys. Rev.*, **104**, 328 (1961).
10) G. A. Sawatzky, F. van der Woude, and A. H. Morrish, *Phys. Lett.*, **31**, 147 (1967).
11) T. Okada, S. Ambe, F. Ambe, and H. Sekizawa, *J. Phys. Chem.*, **86**, 4726 (1982).
12) I. S. Lyubutin, T. Ohya, T. V. Dmitrieva, and K. Ono, *J. Phys. Soc. Jpn.*, **36**, 1006 (1974).
13) F. Grandjian, "Mössbauer Spectroscopy Applied to Inorganic Chemistry," ed by G. J. Long, Plenum Press, New York and London (1987), Vol. 2, p. 241.
14) F. Izumi, "Advances in X-ray Chemical Analysis, Japan, No. 14," Agne, Tokyo (1983), p. 43.
15) F. Izumi, M. Mitomo, and Y. Bando, *J. Mater. Sci.*, **19**, 3115 (1984).
16) J. Hesse and A. Rubartsch, *J. Phys. E.*, **17**, 526 (1974).
17) G. V. Novikov, V. A. Trukhtanov, S. I. Yushchuk, and N. A. Grigoryan, *Sov. Phys. Solid State*, **9**, 2350 (1968).
18) E. D. Grave, A. Govaert, D. Chambaere, and G. Robbrecht, *Physica*, **96B**, 103 (1979).
19) P. P. Bakare, J. J. Shrotri, C. E. Deshpande, M. P. Gupta, and S. D. Date, *India J. Chem.*, **26A**, 1 (1987).
20) V. A. Bokov, G. V. Novikov, Y. G. Saksonov, V. A. Trukhtanov, and S. I. Yushchuk., *Sov. Phys. Solid State*, **16**, 2364 (1975).
21) G. V. Novikov, V. A. Trukhtanov, L. Cser, S. I. Yushchuk, and V. I. Goldanskii, *Sov. Phys. JETP*, **29**, 403 (1969).
22) T. Shigematsu, H. Torii, M. Kiyama, T. Shinjo, and T. Takada, *J. Phys. Soc. Jpn.*, **48**, 689 (1980).